

**IMPROVED MODULATION TECHNIQUES FOR  
MATRIX CONVERTERS AND THEIR APPLICATIONS IN  
INDUCTION MOTOR DRIVES**

**TABISH NAZIR MIR**



**DEPARTMENT OF ELECTRICAL ENGINEERING  
INDIAN INSTITUTE OF TECHNOLOGY DELHI  
NOVEMBER 2020**

© Indian Institute of Technology Delhi (IITD), New Delhi, 2020

**IMPROVED MODULATION TECHNIQUES FOR  
MATRIX CONVERTERS AND THEIR APPLICATIONS IN  
INDUCTION MOTOR DRIVES**

*by*

**TABISH NAZIR MIR**

**Department of Electrical Engineering**

*Submitted*

**in fulfillment of the requirements of the degree of Doctor of Philosophy**

*to the*



**INDIAN INSTITUTE OF TECHNOLOGY DELHI**


**NOVEMBER 2020**

# CERTIFICATE

This is to certify that the thesis entitled ‘**Improved Modulation Techniques for Matrix Converters and their Applications in Induction Motor Drives**’ being submitted by **Ms. Tabish Nazir Mir** for award of the degree of **Doctor of Philosophy** in the Department of Electrical Engineering, Indian Institute of Technology Delhi, is a record of the student work carried out by her under our supervision. The matter embodied in this thesis has not been submitted for award of any other degree or diploma.

**Dated:** November, 2020

(Prof. Bhim Singh)  
Supervisor  
Electrical Engineering Department  
Indian Institute of Technology Delhi  
Hauz Khas, New Delhi-110016, India



(Prof. A. H Bhat)  
Co-Supervisor  
Electrical Engineering Department  
National Institute of Technology Srinagar  
Hazratbal, J&K-190006, India

# ACKNOWLEDGEMENTS

I would like to express my earnest gratitude to my supervisor, **Prof. Bhim Singh** and co-supervisor, **Prof. A.H Bhat**, for their continuous guidance, support and motivation. **Prof. Bhim Singh** has not only been an inspiration, but a guiding light and a visionary mentor. His ingenuity and enthusiasm for research, has been a driving force in keeping me motivated throughout my doctoral studies, and he continues to inspire my career ahead. It has been an exhilarating experience to work under his supervision, and to witness his commitment and passion towards his work. Apart from sharing technical nuances and a multitude of ideas, Prof. Bhim Singh has taught me the importance of discipline, tenacity and perseverance. It has been an absolute honor to learn from him, to be part of his research group, and to do my bit in carrying forward the legacy that he has created. For his teachings, and for his faith in me, I am forever indebted.

The daunting task of pursuing Ph.D. from IIT Delhi and simultaneously serving as faculty at NIT Srinagar, would not have been accomplished without the unflinching support of my supervisor, **Prof. A.H Bhat** at NIT Srinagar. From introducing me to power electronics in my undergraduate studies, to motivating and supporting me throughout my Ph.D. journey, Prof. A.H Bhat has been instrumental in the completion of this thesis. Without the lab infrastructure created by Prof. A.H Bhat at NIT Srinagar, this thesis in its current form would not have been possible. In my moments of despair, it has been Prof. Bhat who has reminded me that there is no substitute for hardwork and that my hardwork shall pay off. For those reminders, and for his unwavering support and guidance, I am forever indebted.

I wish to express my sincere thanks and heartfelt gratitude to all my SRC members, **Prof. Sukumar Mishra**, **Dr. Anandarup Das**, and **Dr. Ashu Verma**, for their valuable inputs, regular guidance and constructive suggestions that have helped in shaping this thesis.

I sincerely thank the Department of Electrical Engineering at NIT Srinagar, for lending financial and laboratory support to my research, especially Prof. S.A Lone and Prof. A.H Bhat, who extended complete financial support during their respective tenures as

Heads of the department. I am eternally grateful to Prof. Bhim Singh, for his financial support towards experimentation at IIT Delhi, conference registrations and article processing charges. My sincere thanks to the lab staff, Mr. Puran Singh, and Mr. Jitender Singh for facilitating my work at PG Machines Lab, IIT Delhi, and Mr. Farooq for his assistance during experimentation at Power Electronics Lab, NIT Srinagar.

Special thanks to my lab mates at IIT Delhi, and colleagues at NIT Srinagar. It has been a pleasure to have the company of Mrs. Subarni Pradhan, Mrs. Nidhi Mishra, Mr. Anshul Varshney, Mr. Utkarsh Sharma, Mrs. Farheen, Mrs. Shubra, Mr. Piyush Kanth, Mrs. Pavitra, Mrs. Rohini, Ms. Hina Parveen, Mrs. Rashmi, Dr. Nishant Kumar, Dr. Aniket Anand, Ms. Yashi, and all juniors and seniors at P.G Machines Lab. A special mention to Mrs. Subarni for being my constant companion and friend at IIT Delhi, and to Mr. Anshul Varshney for being one of the most helpful people in the lab. My deepest gratitude to my friends and colleagues at NIT Srinagar, Dr. Fatima Jalid, Ms. Aravi Muzzaffar, Mrs. Uferah Maqbool, Ms. Iqra, Ms. Falak, Mr. Ved Prakash and Dr. Janib Bashir, who have been partners with me in handling full time teaching while pursuing Ph.D.

So often you find that the students you're trying to inspire, end up inspiring you. A very special mention goes to my dearest students who continue to make me proud, especially those who did their final year B.Tech projects with me, and with whom I shared my struggles, failures and victories at experimental work. My deepest gratitude to Sohaib, Adnan, and Burooj, for sharing my excitement and zeal for matrix converters, and for helping me in experimentation.

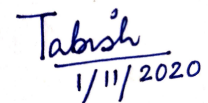
I express my profound gratitude to my parents for their prayers and encouragement. If it wasn't for my father, Mr. Nazir Ahmed Mir, I would not have known sincerity, and it is my mother, Mrs. Masooda Nazir, who taught me endurance. These two virtues have been my guiding stars during this journey. I am eternally grateful to my parents for their incredible support system and my sisters Dr. Mahvish Nazir and Dr. Beenish Nazir for being my biggest cheer leaders.

My deepest appreciation is for my husband, Mr. Aamir Rafiq, for his unfaltering

support towards my dreams and aspirations. His immeasurable patience, love and reassurance, has gone a long way in helping me overcome the difficulties that I encountered during the course of my research. Thank you for always having my back, and for making my dreams, your own.

Finally, my most sincere gratitude to the Almighty, who has known all my moments of joy and despair, and has given me the strength to never say die.

Date: November 2020

Handwritten signature in blue ink that reads "Tabish" with a horizontal line underneath, and the date "1/11/2020" written below the line.

Tabish Nazir Mir

# ABSTRACT

One of the major industrial applications of power electronics, is the control of motor drives, which are mostly dominated by converter fed induction motors. In such applications, features like energy efficiency, improved power quality, high power density and improved reliability are highly desirable. While most three-phase induction motor drives are conventionally fed through AC-DC-AC converters, this traditional approach is associated with a large footprint owing to an intermediate DC stage. DC link capacitor used as an intervening energy storage element, is not only bulky but also contributes to low system reliability. An interesting alternative in the form of matrix converters, has been widely researched over the past two decades. Matrix converter belongs to the breed of direct AC-AC converters, that facilitate multi-phase power conversion with smooth voltage control at unrestricted frequency, without any intervening DC link. It offers advantages such as improved power quality on source as well as load side, inherent bidirectionality, completely controllable input power factor, compact size and possibility for common mode voltage elimination. Owing to these features, matrix converters have been used in motor drives, wind energy conversion systems and aerospace applications.

In spite of a wide range of advantages, the industry acceptability of matrix converters has been limited. This is primarily because of difficulties in control, protection, and commutation. While some of these challenges have been overcome through research, others are still being worked upon. This thesis deals with the design and development of matrix converter fed induction motor drive, with complete protection and multi-step commutation. It elucidates some novel and improved modulation strategies for matrix converters, from the perspective of controlling induction motor drives. For the purpose of controlling three-phase induction motor drive, two topologies are selected viz. three-phase to three-phase matrix converter and single-phase to three-phase matrix converter. The challenges associated with the modulation of each topology are individually addressed, and their suitability is explored in the speed sensor-less control of three-phase induction motor drives.

Three-phase to three-phase matrix converter is the most commonly explored topol-

ogy amongst multi-phase matrix converters. A large number of possible switching states, coupled with the simultaneous control of source and load side parameters, leads to complicated modulation. Space vector modulation remains one of the most popular control techniques which allows concurrent tracing of output voltage and input current space vectors. However, it is associated with high processor burden and complex implementation. Over the past decade, finite control set model predictive control (FCS-MPC) has been explored in the modulation of three-phase to three-phase matrix converter. It has especially shown promising results while achieving multiple objectives of source and load current control. However, it is associated with extensive mathematical modeling of load and input filter, besides performance dependence on processor strength. This thesis deals with certain improved and novel modulation approaches for three-phase to three-phase matrix converter that tend to simplify modulation and control. It deals with an improvised multi-objective model predictive control strategy that combines FCS-MPC and space vector modulation to achieve enhanced system performance at higher sample times and limits switching frequency variations. Furthermore, a unique predictive delta sigma modulation (PDSM) technique is proposed, that is simple and intuitive to implement, with significantly reduced processor burden and enhanced system performance as compared to previously documented techniques. PDSM is also explored in common mode voltage elimination for three-phase to three-phase matrix converter based systems. Speed sensor-less vector control is implemented for commonly used 21 states of the converter using PDSM technique with a full order predictive observer for wide range of speed estimation. Moreover, the matrix converter fed induction motor drive is modulated using only six common mode voltage eliminating states in order to present a more reliable drive solution, while tapping all other advantages of the converter, over a wide range of rotor speed. The speed sensor-less drive is also tested for hysteresis based direct torque control (DTC) and constant switching frequency based DTC, with suitable choice of speed observers. All control algorithms are developed in Matlab/Simulink environment, followed by experimental verification on a four layer PCB prototype of matrix converter based induction motor drive.

In order to facilitate the control of a three-phase induction motor on a single phase supply, the use of single-phase to three-phase matrix converter is advocated. This topology has not garnered significant interest of the research community owing to a poor voltage conversion ratio, and severely compromised harmonic performance due to instantaneous power mismatch between single-phase input and three-phase output. This thesis explores the optimum use of single-phase to three-phase matrix converter for low speed sensor-less control of three-phase induction motor drive from a single-phase supply. The delta sigma technique is demonstrated for enhancement of motor current quality in the low speed region, while compromising on the quality of source current. Further, a multi-objective FCS-MPC technique is demonstrated and compared with other modulation schemes, to achieve a suitable trade-off between the power quality on the grid side versus that on the motor side. All modulation techniques are experimentally validated on single-phase to three-phase matrix converter fed inductive load followed by demonstration with speed sensor-less control on a three-phase induction motor drive.

## सार

पावर इलेक्ट्रॉनिक्स के प्रमुख औद्योगिक अनुप्रयोगों में से एक मोटर ड्राइव का नियंत्रण है, जो ज्यादातर कनवर्टर फेड इंडक्शन मोटर्स द्वारा हावी हैं। ऐसे अनुप्रयोगों में, ऊर्जा दक्षता, बेहतर बिजली की गुणवत्ता, उच्च शक्ति घनत्व और बेहतर विश्वसनीयता जैसी विशेषताएं अत्यधिक वांछनीय हैं। जबकि अधिकांश तीन-चरण प्रेरण मोटर ड्राइव को पारंपरिक रूप से एसी-डीसी-एसी कनवर्टर्स के माध्यम से खिलाया जाता है, यह पारंपरिक दृष्टिकोण एक बड़े पदचिह्न के साथ एक मध्यवर्ती डीसी चरण के कारण जुड़ा हुआ है। डीसी लिंक कैपेसिटर एक हस्तक्षेप ऊर्जा भंडारण तत्व के रूप में उपयोग किया जाता है, न केवल भारी है और कम सिस्टम विश्वसनीयता में भी योगदान देता है। मैट्रिक्स कनवर्टर्स के रूप में एक दिलचस्प विकल्प पिछले दो दशकों में व्यापक रूप से शोध किया गया है। मैट्रिक्स कनवर्टर प्रत्यक्ष एसी-एसी कनवर्टर्स की नस्ल से संबंधित है जो बिना किसी हस्तक्षेप के डीसी लिंक के बिना अप्रतिबंधित आवृत्ति पर चिकनी वोल्टेज नियंत्रण के साथ बहु-चरण बिजली रूपांतरण की सुविधा प्रदान करता है। यह स्रोत पर बेहतर बिजली की गुणवत्ता के साथ-साथ लोड साइड, अंतर्निहित द्वि-दिशात्मकता, पूरी तरह से नियंत्रणीय इनपुट पावर फैक्टर, कॉम्पैक्ट आकार और सामान्य मोड वोल्टेज उन्मूलन की संभावना जैसे लाभ प्रदान करता है। इन विशेषताओं के कारण, मोटर ड्राइव, पवन ऊर्जा रूपांतरण प्रणाली और एयरोस्पेस अनुप्रयोगों में मैट्रिक्स कनवर्टर्स का उपयोग किया गया है

कई प्रकार के लाभों के बावजूद, मैट्रिक्स कनवर्टर्स की उद्योग स्वीकार्यता सीमित हो गई है। यह मुख्य रूप से नियंत्रण, सुरक्षा और आवागमन में कठिनाइयों के कारण है। हालांकि इनमें से कुछ चुनौतियों को अनुसंधान के माध्यम से दूर किया गया है, लेकिन अभी भी दूसरों पर काम किया जा रहा है। यह थीसिस पूरी तरह से सुरक्षा और मल्टी-स्टेप कन्वर्शन के साथ मैट्रिक्स कनवर्टर फेड इंडक्शन मोटर ड्राइव के डिजाइन और विकास से संबंधित है। यह प्रेरण मोटर ड्राइव को नियंत्रित करने के दृष्टिकोण से, मैट्रिक्स कनवर्टर्स के लिए कुछ उपन्यास और बेहतर मॉड्यूलेशन रणनीतियों को स्पष्ट करता है। तीन-चरण प्रेरण मोटर ड्राइव को नियंत्रित करने के उद्देश्य से, दो टोपोलॉजीज़ का चयन किया जाता है। तीन-चरण मैट्रिक्स कनवर्टर के लिए तीन-चरण और तीन-चरण मैट्रिक्स कनवर्टर के लिए एकल-चरण। प्रत्येक टोपोलॉजी के मॉड्यूलेशन से जुड़ी चुनौतियों को व्यक्तिगत रूप से संबोधित किया जाता है, और तीन-चरण प्रेरण मोटर ड्राइव के स्पीड सेंसर-कम नियंत्रण में उनकी उपयुक्तता का पता लगाया जाता है।

तीन-चरण से तीन-चरण मैट्रिक्स कनवर्टर बहु-चरण मैट्रिक्स कनवर्टर्स के बीच सबसे अधिक खोजा गया टोपोलॉजी है। स्रोत और लोड साइड मापदंडों के एक साथ नियंत्रण के साथ मिलकर संभव स्विचिंग राज्यों की एक बड़ी संख्या, जटिल मॉड्यूलेशन की ओर ले जाती है। स्पेस वेक्टर मॉड्यूलन सबसे लोकप्रिय नियंत्रण तकनीकों में से एक बना हुआ है जो आउटपुट वोल्टेज और इनपुट करंट स्पेस वेक्टर के समवर्ती अनुरेखण की अनुमति देता है। हालांकि, यह उच्च प्रोसेसर बोझ और जटिल कार्यान्वयन से जुड़ा हुआ है। पिछले एक दशक में, तीन चरण के तीन-चरण मैट्रिक्स कनवर्टर के मॉड्यूलेशन में परिमित नियंत्रण सेट मॉडल भविष्य कहनेवाला नियंत्रण (एफसीएस-एमपीसी) का पता लगाया गया है। स्रोत के कई उद्देश्यों को प्राप्त करते हुए और वर्तमान नियंत्रण को लोड करते हुए इसने विशेष रूप से आशाजनक परिणाम दिखाए हैं। हालांकि, यह लोड और इनपुट फिल्टर

के व्यापक गणितीय मॉडलिंग के साथ जुड़ा हुआ है, इसके अलावा प्रोसेसर की ताकत पर प्रदर्शन निर्भरता है। यह थीसिस तीन-चरण से तीन-चरण मैट्रिक्स कन्वर्टर के लिए कुछ बेहतर और उपन्यास मॉड्यूलेशन दृष्टिकोणों से संबंधित है जो मॉड्यूलेशन और नियंत्रण को सरल बनाते हैं। यह एक इंप्रूव्ड मल्टी-ऑब्जेक्टिव मॉडल प्रेडिक्टिव कंट्रोल स्ट्रैटेजी के साथ है जो एफसीएस-एमपीसी और स्पेस वेक्टर मॉड्यूलेशन को बढ़ाकर उच्च नमूना समय पर सिस्टम प्रदर्शन को प्राप्त करने और आवृत्ति भिन्नताओं को स्विच करने को सीमित करता है। इसके अलावा, एक अद्वितीय भविष्य कहनेवाला सिग्मा सिग्मा मॉड्यूलेशन (PDSM) तकनीक प्रस्तावित है, जो सरल और सहज जान युक्त है, जिसमें पहले से ही प्रलेखित तकनीकों की तुलना में काफी कम प्रोसेसर बोझ और बढ़ा हुआ सिस्टम प्रदर्शन है। PDSM भी तीन चरण तीन चरण मैट्रिक्स कन्वर्टर आधारित प्रणालियों के लिए आम मोड वोल्टेज उन्मूलन में पता लगाया है। गति संवेदक-कम वेक्टर नियंत्रण आमतौर पर उपयोग किए जाने वाले कन्वर्टर के 21 राज्यों के लिए लागू किया जाता है, जो पीडीएस तकनीक का उपयोग करते हुए गति अनुमानों की विस्तृत श्रृंखला के लिए एक पूर्ण ऑर्डर प्रेडिक्टिव ऑब्जेक्टिव है। इसके अलावा, रोटर गति की एक विस्तृत श्रृंखला में, कन्वर्टर के अन्य सभी लाभों का दोहन करते हुए, एक और अधिक विश्वसनीय ड्राइव समाधान पेश करने के लिए मैट्रिक्स कन्वर्टर फेड इंडक्शन मोटर ड्राइव को केवल छह सामान्य मोड वोल्टेज को नष्ट करने वाले राज्यों का उपयोग करके संशोधित किया जाता है। गति पर्यवेक्षक की उपयुक्त पसंद के साथ गति संवेदक-आधारित ड्राइव का परीक्षण हिस्टैरिसिस आधारित प्रत्यक्ष टोक नियंत्रण (डीटीसी) और निरंतर स्विचिंग आवृत्ति आधारित डीटीसी के लिए भी किया जाता है। सभी नियंत्रण एल्गोरिदम Matlab / Simulink वातावरण में विकसित किए जाते हैं, इसके बाद मैट्रिक्स कन्वर्टर आधारित इंडक्शन मोटर ड्राइव के चार परत पीसीबी प्रोटोटाइप पर प्रायोगिक सत्यापन किया जाता है।

एकल चरण आपूर्ति पर तीन-चरण प्रेरण मोटर के नियंत्रण की सुविधा के लिए, एकल-चरण से तीन-चरण मैट्रिक्स कन्वर्टर का उपयोग करने की वकालत की जाती है। इस टोपोलॉजी ने खराब वोल्टेज रूपांतरण अनुपात के कारण अनुसंधान समुदाय के महत्वपूर्ण हित को प्रभावित नहीं किया है, और एकल-चरण इनपुट और तीन-चरण आउटपुट के बीच तात्कालिक बिजली बेमेल के कारण गंभीर रूप से समझौता हार्मोनिक प्रदर्शन किया है। यह थीसिस एकल-चरण आपूर्ति से तीन-चरण प्रेरण मोटर ड्राइव के कम गति सेंसर-कम नियंत्रण के लिए एकल-चरण से तीन-चरण मैट्रिक्स कन्वर्टर के इष्टतम उपयोग की पड़ताल करता है। डेल्टा सिग्मा तकनीक का उत्पादन कम गति वाले क्षेत्र में मोटर करंट क्वालिटी को बढ़ाने के लिए किया जाता है, जबकि स्रोत की गुणवत्ता पर समझौता किया जाता है। इसके अलावा, एक बहुउद्देश्यीय एफसीएस-एमपीसी तकनीक का प्रदर्शन और अन्य मॉड्यूलन योजनाओं के साथ तुलना में किया जाता है, ताकि मोटर साइड पर ग्रिड की तरह बिजली की गुणवत्ता के बीच एक उपयुक्त व्यापार बंद प्राप्त किया जा सके। सभी मॉड्यूलेशन तकनीकों को एकल-चरण से लेकर तीन-चरण मैट्रिक्स कन्वर्टर में आगमनात्मक भार के साथ तीन-चरण प्रेरण मोटर ड्राइव पर गति सेंसर-कम नियंत्रण के साथ मान्य किया गया है।

# Table of Contents

|   |           |
|---|-----------|
| List of Figures   | xviii     |
| List of Tables  | xxx       |
| <b>CHAPTER I INTRODUCTION</b>   | <b>1</b>  |
| 1.1 General   | 1         |
| 1.2 State of Art on Static AC-AC Power Conversion   | 2         |
| 1.2.1 AC-DC-AC Converters   | 2         |
| 1.2.2 Cyclo-Converters  | 3         |
| 1.2.3 Matrix Converters   | 4         |
| 1.3 Objectives and Scope of Work  | 7         |
| 1.4 Outline of Chapters   | 9         |
| <b>CHAPTER II LITERATURE REVIEW</b>   | <b>13</b> |
| 2.1 General   | 13        |
| 2.2 Literature Survey   | 13        |
| 2.2.1 Review of Matrix Converter Topologies   | 14        |
| 2.2.1.1 Three Phase to Three Phase Matrix Converters  | 14        |
| 2.2.1.2 Single Phase to Three Phase Matrix Converters   | 16        |
| 2.2.2 Review of Modulation Strategies for Matrix Converters   | 18        |
| 2.2.2.1 Venturini-Alesini Algorithm for Matrix Converters   | 19        |
| 2.2.2.2 Scalar Control Algorithm for Matrix Converters  | 20        |
| 2.2.2.3 Space Vector Modulation for Matrix Converters   | 20        |
| 2.2.2.4 Model Predictive Control for Matrix Converters  | 21        |
| 2.2.3 Review of Protection and Commutation Techniques for Bi-Directional<br>Devices Used in Matrix Converters | 22        |
| 2.2.4 Review of Matrix Converter Fed Induction Motor Drives   | 24        |
| 2.2.5 Review of Sensor-less Control of Induction Motor Drives   | 25        |
| 2.3 Identified Research Areas   | 26        |
| 2.4 Conclusions   | 27        |
| <b>CHAPTER III CLASSIFICATION, CONFIGURATIONS AND DE-<br/>SIGN OF MATRIX CONVERTERS</b>                       | <b>28</b> |
| 3.1 General   | 28        |
| 3.2 Classification of Matrix Converter Topologies   | 28        |
| 3.3 Configurations of Matrix Converter Topologies   | 29        |

|       |  |    |
|-------|--|----|
| 3.3.1 | Three Phase to Three Phase Matrix Converter Fed Induction Motor Drive  | 29 |
| 3.3.2 | Single-Phase to Three-Phase Matrix Converter Fed Induction Motor Drive | 30 |
| 3.4   | Design and Implementation  | 30 |
| 3.4.1 | Design and Layout of Power Circuit                                     | 31 |
| 3.4.2 | Design and Layout of Gate Driver Circuits                              | 32 |
| 3.4.3 | Design and Implementation of Input Filter                              | 32 |
| 3.4.4 | System Auxiliaries   | 34 |
|       | 3.4.4.1 Signal Conditioning Circuit for Voltage Sensors                | 34 |
|       | 3.4.4.2 Signal Conditioning Circuit for Current Sensors                | 35 |
| 3.5   | Selection of Induction Motor   | 35 |
| 3.6   | Protection Issues in Matrix Converter                                  | 36 |
| 3.6.1 | FPGA implementation of Four Step Commutation                           | 37 |
| 3.6.2 | Design of Clamp Circuit  | 38 |
| 3.7   | Execution of Control Algorithm using dSPACE RTI 1202                   | 39 |
| 3.8   | Integrated Hardware Setup  | 40 |
| 3.9   | Results and Discussion   | 41 |
| 3.9.1 | Test Results of Four Step Commutation                                  | 41 |
| 3.9.2 | Test Results of Voltage and Current Sensing Units                      | 43 |
| 3.9.3 | Test Results of Space Vector Modulation for Matrix Converter           | 43 |
| 3.10  | Conclusions  | 44 |

## **CHAPTER IV IMPROVED MODULATION TECHNIQUES FOR MATRIX CONVERTERS** **45**

|         |   |    |
|---------|---|----|
| 4.1     | General   | 45 |
| 4.2     | Configuration of Three-Phase to Three-Phase Matrix Converter Fed Inductive Load             | 46 |
| 4.3     | Requirements of Modulation Techniques for Matrix Converters                                 | 47 |
| 4.4     | Modulation Techniques for Matrix Converters   | 48 |
| 4.4.1   | Multi-objective Finite Control Set Model Predictive Control (FCS-MPC) for Matrix Converters | 49 |
|         | 4.4.1.1 Classical Multi-objective FCS-MPC for Matrix Converter                              | 49 |
|         | 4.4.1.1.1 Mathematical Modeling of Load   | 50 |
|         | 4.4.1.1.2 Mathematical Modeling of Input Filter   | 50 |
|         | 4.4.1.1.3 Weight Selection and Minimization of Cost Function                                | 52 |
|         | 4.4.1.1.4 Limitations of Classical Multi-objective FCS-MPC                                  | 52 |
| 4.4.1.2 | Fuzzy Decision Making (FDM) for Elimination of Weighing Factors                             | 53 |

|           |   |    |
|-----------|---|----|
| 4.4.1.3   | Improved Switching Implementation by Incorporating Space Vector Modulation (SVM) in Fuzzy Decision Making (FDM)                                     | 54 |
| 4.4.2     | Predictive Delta Sigma Modulation for Matrix Converters   | 56 |
| 4.4.2.1   | Load Voltage Control  | 58 |
| 4.4.2.2   | Source Current Control  | 59 |
| 4.4.2.2.1 | Generation of Source Current Reference  | 59 |
| 4.4.2.2.2 | Load Current Prediction for Source Current Control  | 60 |
| 4.4.2.3   | Development of the Final Switching Scheme   | 62 |
| 4.4.2.4   | Design of Integrator Gains, $k_v$ and $k_i$   | 63 |
| 4.4.2.5   | Effect of Hysteresis Band   | 64 |
| 4.4.3     | Predictive Delta Sigma Modulation for Common Mode Voltage (CMV) Elimination in Matrix Converters  | 65 |
| 4.4.3.1   | Load Voltage Control for CMV Elimination  | 67 |
| 4.4.3.2   | Source Current Control for CMV Elimination  | 68 |
| 4.4.3.3   | Final Switching   | 69 |
| 4.5       | MATLAB Based Modeling and Simulation of Three-Phase to Three-Phase Matrix Converter Fed Inductive Load  | 71 |
| 4.6       | Hardware Implementation of Three-Phase to Three-Phase Matrix Converter Fed Inductive Load   | 72 |
| 4.7       | Results and Discussion  | 72 |
| 4.7.1     | Performance of Improved Switching Implementation for Matrix Converter by incorporating Space Vector Modulation (SVM) in Fuzzy Decision Making (FDM) | 73 |
| 4.7.1.1   | Load Side Performance   | 74 |
| 4.7.1.2   | Source Side Performance   | 75 |
| 4.7.1.3   | Power Quality Performance   | 76 |
| 4.7.2     | Performance of Predictive Delta Sigma Modulation for Matrix Converter   | 79 |
| 4.7.2.1   | Dynamic Performance   | 80 |
| 4.7.2.2   | Steady State Performance  | 82 |
| 4.7.2.3   | Power Quality Performance   | 83 |
| 4.7.3     | Performance of Predictive Delta Sigma Modulation for CMV Elimination in Matrix Converter  | 84 |
| 4.7.3.1   | Dynamic Performance   | 85 |
| 4.7.3.2   | Steady State Performance  | 86 |
| 4.7.3.3   | Power Quality Performance   | 88 |
| 4.7.4     | Comparative Analysis of Modulation Techniques   | 90 |
| 4.8       | Conclusions   | 92 |

## **CHAPTER V SPEED SENSOR-LESS VECTOR CONTROL OF THREE-PHASE TO THREE-PHASE MATRIX CONVERTER FED INDUCTION MOTOR DRIVE** **95**

|     |         |    |
|-----|---------|----|
| 5.1 | General | 95 |
|-----|---------|----|

|           |  |     |
|-----------|--|-----|
| 5.2       | Configuration of Three-Phase to Three-Phase Matrix Converter Fed Induction Motor Drive   | 95  |
| 5.3       | Vector Control of Three-Phase to Three-Phase Matrix Converter Fed Induction Motor Drive  | 96  |
| 5.3.1     | Speed Sensor-less Vector Control of Three-Phase to Three-Phase Matrix Converter Fed Induction Motor Drive Using Conventional 21 States                   | 97  |
| 5.3.1.1   | State Estimation Using Model Predictive Control  | 98  |
| 5.3.1.2   | Control and Modulation   | 102 |
| 5.3.1.2.1 | Flux and Speed Control   | 102 |
| 5.3.1.2.2 | Input-Output Power Balance   | 103 |
| 5.3.1.2.3 | Delta Sigma Modulation   | 104 |
| 5.3.2     | Speed Sensor-less Vector Control of Three-Phase to Three-Phase Matrix Converter Fed Induction Motor Drive Using 6 Common Mode Voltage Eliminating States | 105 |
| 5.3.2.1   | Multi-Objective FCS-MPC of Matrix Converter Fed Induction Motor With Zero CMV  | 109 |
| 5.3.2.1.1 | Mathematical Modeling of Induction Motor for Stator Current Prediction   | 109 |
| 5.3.2.1.2 | Modeling of Input Filter for Source Current Prediction   | 111 |
| 5.3.2.1.3 | State Selection Using Fuzzy Normalization  | 112 |
| 5.3.2.2   | State Estimation and Control   | 114 |
| 5.3.2.2.1 | Estimation of Rotor Flux and Rotor Speed   | 114 |
| 5.3.2.2.2 | Generation of Stator and Source Current References   | 116 |
| 5.4       | MATLAB Based Modeling and Simulation for Speed Sensor-less Vector Control of Three-Phase to Three-Phase Matrix Converter Fed Induction Motor Drive       | 117 |
| 5.5       | Hardware Implementation for Speed Sensor-less Vector Control of Three-Phase to Three-Phase Matrix Converter Fed Induction Motor Drive                    | 118 |
| 5.6       | Results and Discussion   | 119 |
| 5.6.1     | Performance of Speed Sensor-less Vector Control for Three-Phase to Three-Phase Matrix Converter Fed Induction Motor Drive Using Conventional 21 States   | 119 |
| 5.6.1.1   | Starting Performance   | 120 |
| 5.6.1.2   | Dynamics During Speed Control and Reversal   | 120 |
| 5.6.1.3   | Dynamics During Load Perturbation  | 122 |
| 5.6.1.4   | Steady state Performance   | 122 |
| 5.6.1.5   | Power Quality Performance  | 124 |
| 5.6.2     | Performance of Speed Sensor-less Vector Control for Three-Phase to Three-Phase Matrix Converter Fed Induction Motor Drive with Zero CMV                  | 124 |
| 5.6.2.1   | Starting Performance   | 125 |

|         |   |     |
|---------|---|-----|
| 5.6.2.2 | Dynamics During Speed Control and Reversal  | 126 |
| 5.6.2.3 | Dynamics During Load Perturbation           | 128 |
| 5.6.2.4 | Steady State Performance                    | 129 |
| 5.6.2.5 | Power Quality Performance                   | 129 |
| 5.6.2.6 | Performance in terms of Common Mode Voltage | 130 |
| 5.6.2.7 | Comparative Assessment                      | 132 |
| 5.6.3   | Design of Control Gains                     | 133 |
| 5.7     | Conclusions                                 | 135 |

## **CHAPTER VI SPEED SENSOR-LESS DIRECT TORQUE CONTROL OF THREE-PHASE TO THREE-PHASE MATRIX CONVERTER FED INDUCTION MOTOR DRIVE** **137**

|           |   |     |
|-----------|---|-----|
| 6.1       | General   | 137 |
| 6.2       | Configuration of Three-Phase to Three-Phase Matrix Converter Fed Induction Motor Drive  | 138 |
| 6.3       | Direct Torque Control of Three-Phase to Three-Phase Matrix Converter Fed Induction Motor Drive  | 138 |
| 6.3.1     | Speed Sensor-less DTC of Three-Phase to Three-Phase Matrix Converter Fed Induction Motor Drive  | 139 |
| 6.3.1.1   | DTC Through Matrix Converter  | 140 |
| 6.3.1.2   | Input Power Factor Control  | 142 |
| 6.3.1.3   | Speed Sensor-less Operation Through Adaptive Flux Observer  | 144 |
| 6.3.1.3.1 | Modeling of Induction Motor   | 145 |
| 6.3.1.3.2 | Adaptive Flux Observer  | 146 |
| 6.3.2     | Constant Switching Frequency DTC for Three-Phase to Three-Phase Matrix Converter Fed Speed Sensor-less Induction Motor Drive            | 147 |
| 6.3.2.1   | State Estimation  | 149 |
| 6.3.2.1.1 | Stator Voltage, Flux and Torque Estimation  | 149 |
| 6.3.2.1.2 | MRAS based Speed Estimation   | 150 |
| 6.3.2.2   | DTC at Constant Switching Frequency   | 151 |
| 6.3.2.3   | SVM of MC with Input Power Factor Correction  | 154 |
| 6.4       | MATLAB Based Modeling and Simulation for Speed Sensor-less DTC of Three-Phase to Three-Phase Matrix Converter Fed Induction Motor Drive | 156 |
| 6.5       | Hardware Implementation for Speed Sensor-less DTC of Three-Phase to Three-Phase Matrix Converter Fed Induction Motor Drive              | 156 |
| 6.6       | Results and Discussion  | 158 |
| 6.6.1     | Performance of Speed Sensor-less DTC for Three-Phase to Three-Phase Matrix Converter Fed Induction Motor Drive                          | 158 |
| 6.6.1.1   | Starting Performance  | 158 |

|  |   |            |
|--|---|------------|
| 6.6.1.2  | Dynamics During Speed Reversal  | 159        |
| 6.6.1.3  | Dynamics During Load/Source Perturbation  | 160        |
| 6.6.1.4  | Steady State Performance  | 161        |
| 6.6.1.5  | Power Quality Performance   | 163        |
| 6.6.2  | Performance of Constant Switching Frequency DTC for Three-Phase to Three-Phase Matrix Converter Fed Induction Motor Drive with Zero CMV             | 165        |
| 6.6.2.1  | Starting Performance  | 165        |
| 6.6.2.2  | Dynamics During Speed Reversal  | 167        |
| 6.6.2.3  | Steady State Performance  | 167        |
| 6.6.3  | Comparative Analysis of Constant Switching DTC with Conventional DTC  | 169        |
| 6.7  | Conclusions   | 170        |
| <b>CHAPTER VII LOAD ORIENTED CONTROL OF SINGLE-PHASE TO THREE-PHASE MATRIX CONVERTER FED INDUCTION MOTOR DRIVE</b> |   | <b>172</b> |
| 7.1  | General   | 172        |
| 7.2  | Configuration of Single-Phase to Three-Phase Matrix Converter Fed Induction Motor Drive   | 173        |
| 7.3  | Low Speed Sensor-less Load Oriented Control of Single-Phase to Three-Phase Matrix Converter Fed Induction Motor Drive                               | 174        |
| 7.3.1  | Delta Sigma Modulation for Load Side Power Quality Improvement in Single-Phase to Three-Phase Matrix Converter                                      | 174        |
| 7.3.2  | Full Order Predictive Observer for State Estimation   | 177        |
| 7.3.3  | Speed Sensor-less Control   | 178        |
| 7.4  | MATLAB Based Modeling and Simulation for Speed Sensor-less Vector Control of Single-Phase to Three-Phase Matrix Converter Fed Induction Motor Drive | 178        |
| 7.5  | Hardware Implementation for Speed Sensor-less Vector Control of Single-Phase to Three-Phase Matrix Converter Fed Induction Motor Drive              | 179        |
| 7.6  | Results and Discussion  | 180        |
| 7.6.1  | Performance of Delta Sigma Modulation for Single-Phase to Three-Phase Matrix Converter  | 181        |
| 7.6.1.1  | Dynamic Performance   | 181        |
| 7.6.1.2  | Steady State Performance  | 182        |
| 7.6.1.3  | Power Quality Performance   | 184        |
| 7.6.2  | Performance of Speed Sensor-less Vector Control for Single-Phase to Three-Phase Matrix Converter Fed Induction Motor Drive                          | 185        |
| 7.6.2.1  | Starting Performance  | 186        |
| 7.6.2.2  | Dynamics During Speed Control and Reversal  | 187        |
| 7.6.2.3  | Dynamics During Load Perturbation   | 187        |

|   |   |            |
|---|---|------------|
| 7.6.2.4   | Steady State Performance  | 190        |
| 7.6.2.5   | Power Quality Performance   | 190        |
| 7.7   | Conclusions   | 192        |
| <b>CHAPTER VIII MULTI-OBJECTIVE PREDICTIVE CONTROL FOR SINGLE-PHASE TO THREE-PHASE MATRIX CONVERTER</b> |   | <b>194</b> |
| 8.1   | General   | 194        |
| 8.2   | Configuration of Single-Phase to Three-Phase Matrix Converter Fed Induction Motor Drive   | 196        |
| 8.3   | Modulation of 1- $\phi$ TO 3- $\phi$ Matrix Converter   | 197        |
| 8.4   | Finite Control Set Model Predictive Control for 1- $\phi$ TO 3- $\phi$ Matrix Converter   | 199        |
| 8.4.1   | Load Oriented FCS-MPC for 1- $\phi$ TO 3- $\phi$ Matrix Converter   | 200        |
| 8.4.2   | Compromise Between Load and Source Current Quality Using Multi-Objective FCS-MPC  | 201        |
| 8.5   | Speed Sensor-less Multi-Objective FCS-MPC for 1- $\phi$ TO 3- $\phi$ Matrix Converter fed induction motor drive                                     | 202        |
| 8.6   | MATLAB Based Modeling and Simulation for Speed Sensor-less Vector Control of Single-Phase to Three-Phase Matrix Converter Fed Induction Motor Drive | 203        |
| 8.7   | Hardware Implementation for Speed Sensor-less Vector Control of Single-Phase to Three-Phase Matrix Converter Fed Induction Motor Drive              | 204        |
| 8.8   | Results and Discussion  | 204        |
| 8.8.1   | Comparative Analysis of Modulation Techniques for Single-Phase to Three-Phase Matrix Converter  | 205        |
| 8.8.1.1   | Dynamic Performance   | 205        |
| 8.8.1.2   | Steady State Performance  | 207        |
| 8.8.1.3   | Power Quality Performance   | 209        |
| 8.8.2   | Performance of MO-FCS-MPC Based Single-Phase to Three-Phase Matrix Converter Fed Speed Sensor-less Induction Motor Drive                            | 210        |
| 8.8.2.1   | Starting Performance  | 211        |
| 8.8.2.2   | Dynamic Performance   | 211        |
| 8.8.2.3   | Steady State Performance  | 212        |
| 8.8.2.4   | Power Quality Performance   | 212        |
| 8.9   | Conclusions   | 215        |

|   |            |
|---|------------|
| <b>CHAPTER IX MAIN CONCLUSIONS AND SUGGESTIONS FOR FURTHER WORK</b> | <b>218</b> |
| 9.1 General   | 218        |
| 9.2 Main Conclusions  | 219        |
| 9.3 Suggestions for Further Work                                    | 221        |
| <br>  |            |
| <b>REFERENCES</b>   | <b>223</b> |
| <br>  |            |
| <b>LIST OF PUBLICATIONS</b>   | <b>240</b> |
| <br>  |            |
| <b>APPENDIX</b>   | <b>242</b> |
| <br>  |            |
| <b>BIODATA</b>  | <b>245</b> |

# List of Figures

|            |  |    |
|------------|--|----|
| Figure 1.1 | Conventional two stage AC-DC-AC converter fed induction motor drive  | 3  |
| Figure 1.2 | Single stage three-phase to three-phase half wave cycloconverter fed induction motor drive   | 4  |
| Figure 1.3 | Three-phase to three-phase matrix converter fed induction motor drive  | 5  |
| Figure 1.4 | Diagrammatic overview of work  | 9  |
| Figure 2.1 | Different configurations of bi-directional devices; (a) Common-Collector configuration (b) Common-emitter configuration (c) Four diodes and one IGBT in a bridge (d) Reverse blocking IGBTs in antiparallel. | 23 |
| Figure 3.1 | Circuit configuration of 3- $\phi$ to 3- $\phi$ matrix converter fed induction motor drive   | 30 |
| Figure 3.2 | Circuit configuration of 1- $\phi$ to 3- $\phi$ matrix converter fed induction motor drive   | 31 |
| Figure 3.3 | Four layer PCB design of matrix converter prototype; (a) PCB Layer 1 (b) PCB Layer 2 (c) PCB Layer 3 (d) PCB Layer 4.  | 32 |
| Figure 3.4 | Four layer PCB design of gate driver circuits; (a) PCB Layer 1 (b) PCB Layer 2 (c) PCB Layer 3 (d) PCB Layer 4.  | 33 |
| Figure 3.5 | Signal conditioning circuit for voltage sensor <i>LEM LV25P</i>  | 35 |
| Figure 3.6 | Signal conditioning circuit for current sensor <i>LEM LA55P</i>  | 36 |
| Figure 3.7 | Illustration of four step commutation technique for positive current   | 38 |
| Figure 3.8 | Matrix converter enabled with over-voltage protection through clamp circuit  | 40 |
| Figure 3.9 | Four layer PCB design of clamp circuit; (a) PCB Layer 1 (b) PCB Layer 2 (c) PCB Layer 3 (d) PCB Layer 4.   | 41 |

|             |   |    |
|-------------|---|----|
| Figure 3.10 | Picture of the complete experimental setup  | 42 |
| Figure 3.11 | Experimental verification of four step commutation; (a) For devices carrying positive current (b) For devices carrying negative current.  | 42 |
| Figure 3.12 | Test results for sensing units; (a) Test result for voltage transducer (b) Test result for current transducer.  | 43 |
| Figure 3.13 | Test results for space vector modulation; (a) Load side response (b) Source side response.  | 44 |
| Figure 4.1  | $3\phi$ - $3\phi$ (ABC-abc) matrix converter fed inductive ( $RL$ ) load  | 46 |
| Figure 4.2  | Reference output voltage ( $v_{abc}^*$ ) and reference input current ( $i_{ABC}^*$ ) space vector diagrams in a $3\phi$ - $3\phi$ MC  | 55 |
| Figure 4.3  | Complete block diagram for the implementation of improvised Mo-FCS-MPC using fuzzy logic and sector information from space vectors  | 56 |
| Figure 4.4  | Block diagram representation of the complete modulation algorithm   | 63 |
| Figure 4.5  | Hysteresis control of integrator outputs  | 63 |
| Figure 4.6  | Signal chasing for; (a) $H = \pm 0.01$ (b) $H = \pm 0.1$  | 65 |
| Figure 4.7  | Minimum switching transitions per state change; (a) Conventional Group-I and Group-II vectors (at least one transition) (b) Group-III vectors for zero CMV (at least two transitions)         | 66 |
| Figure 4.8  | MATLAB/Simulink modeling for implementation of improved FCS-MPC using fuzzy normalization and space vector information for switching decisions  | 71 |
| Figure 4.9  | MATLAB/Simulink modeling for implementation of predictive delta sigma modulation  | 72 |
| Figure 4.10 | Experimental setup for validation of proposed modulation techniques using inductive load  | 73 |
| Figure 4.11 | Simulated results for load voltage ( $v_{ab}$ ) and $3 - \phi$ load currents ( $i_{abc}$ ) for (a) conventional FDM (b) Load voltage and $3 - \phi$ load currents for improvised FDM with SVM | 74 |

|             |   |    |
|-------------|---|----|
| Figure 4.12 | Experimental waveforms of Load voltage ( $v_{ab}$ ) and 3- $\phi$ load currents ( $i_{abc}$ ) for (a) conventional FDM (b) Load voltage and 3- $\phi$ load currents for improvised FDM with SVM       | 75 |
| Figure 4.13 | Source voltage ( $v_A$ ), unfiltered source current ( $i_A$ ) and filtered source current ( $i_{sA}$ ); (a) conventional FDM (b) improvised FDM with SVM  | 76 |
| Figure 4.14 | Experimental waveforms of source voltage ( $v_A$ ), unfiltered source current ( $i_A$ ) and filtered source current ( $i_a$ ) for (a) conventional FDM (b) improvised FDM with SVM                    | 76 |
| Figure 4.15 | Simulated harmonic spectrum of load current ( $i_a$ ); (a) conventional FDM (b) improvised FDM with SVM   | 77 |
| Figure 4.16 | Experimental harmonic spectrum of load current ( $i_{sA}$ ) in (a) conventional FDM (b) improvised FDM with SVM   | 77 |
| Figure 4.17 | Simulated harmonic spectrum of filtered source current ( $i_{sA}$ ); (a) conventional FDM (b) improvised FDM with SVM   | 78 |
| Figure 4.18 | Experimental harmonic spectrum of filtered source ( $i_{sA}$ ) in (a) conventional FDM (b) improvised FDM with SVM  | 78 |
| Figure 4.19 | Simulated dynamic performance during load frequency change for PDSM technique; (a) Load voltage and 3 $\phi$ load currents (b) Source voltage, reference and filtered source current.                 | 81 |
| Figure 4.20 | Simulated dynamic performance during load amplitude change for PDSM technique; (a) Load voltage and 3 $\phi$ load currents (b) Source voltage, reference and filtered source current.                 | 81 |
| Figure 4.21 | Experimental waveforms of dynamic performance during load frequency change for PDSM technique; (a) Load voltage and 3 $\phi$ load currents (b) Source voltage, reference and filtered source current. | 82 |
| Figure 4.22 | Experimental waveforms of dynamic performance during load amplitude change for PDSM technique; (a) Load voltage and 3 $\phi$ load currents (b) Source voltage, reference and filtered source current. | 82 |

|   |    |
|---|----|
| Figure 4.23 Simulated steady state performance for PDSM technique; (a) Load voltage and $3\phi$ load currents (b) Source voltage, unfiltered and filtered source current.                             | 83 |
| Figure 4.24 Experimental waveforms of system steady state performance for PDSM technique; (a) Load voltage and $3\phi$ load currents (b) Source voltage, unfiltered and filtered source current.      | 83 |
| Figure 4.25 Simulated harmonic performance for PDSM technique; (a) Harmonic spectrum of load current (b) Harmonic spectrum of filtered source current.  | 84 |
| Figure 4.26 Experimental harmonic performance for PDSM technique; (a) Harmonic spectrum of load current (b) Harmonic spectrum of filtered source current.   | 84 |
| Figure 4.27 Simulation based dynamic performance of the proposed algorithm; (a) Change in frequency of reference load voltage (b) Change in magnitude of reference load voltage                       | 86 |
| Figure 4.28 Experimental assessment of system dynamic performance; (a) Change in frequency of reference load voltage (b) Change in magnitude of reference load voltage                                | 86 |
| Figure 4.29 Simulated performance of delta sigma modulation for Group-III vectors; (a) Load voltage control (b) Source current control  | 87 |
| Figure 4.30 Steady state performance of DSM based MC for CMV elimination; (a) Load voltage and three-phase load currents (b) Source voltage, unfiltered and filtered source current at near unity IPF | 87 |
| Figure 4.31 Experimental depiction of predictive delta sigma modulation for CMV elimination; (a) Load voltage control (b) Source current control  | 88 |
| Figure 4.32 Experimental waveforms is steady state of PDSM technique for CMV elimination; (a) Load voltage and three-phase load currents (b) Source voltage, unfiltered andf filtered source currents | 88 |

|   |     |
|---|-----|
| Figure 4.33 Harmonic performance of DSM based MC; (a) Harmonic spectrum of load current ( $i_a$ ) (b) Harmonic spectrum of filtered source current ( $i_{sA}$ ) | 89  |
| Figure 4.34 Harmonic analysis (a) Harmonic spectrum of load current (b) Harmonic spectrum of source current   | 89  |
| Figure 4.35 Comparative analysis of source and load side current quality (a) Space Vector Modulation (b) Mo-FCS-MPC (a) Proposed PDSM.                          | 91  |
| Figure 4.36 Output phase voltages and resulting common mode voltage; (a) Using conventional 21 states (b) Using the DSM scheme with only Group-III vectors      | 91  |
| Figure 5.1 $3\phi$ - $3\phi$ (ABC-abc) matrix converter fed induction motor drive   | 96  |
| Figure 5.2 Block diagrammatic representation for speed sensor-less vector control of $3\phi$ IMD using conventional 21 states of matrix converter               | 106 |
| Figure 5.3 Implementation of MO-FS-MPC with Fuzzy Normalized Errors   | 113 |
| Figure 5.4 Block diagrammatic representation for speed sensor-less vector control of $3\phi$ IMD using 6 CMV eliminating states of matrix converter             | 117 |
| Figure 5.5 MATLAB/Simulink modeling for speed sensor-less vector control of $3\phi$ IMD using conventional 21 states of matrix converter                        | 118 |
| Figure 5.6 MATLAB/Simulink modeling for speed sensor-less vector control of $3\phi$ IMD using 6 CMV eliminating states of matrix converter                      | 119 |
| Figure 5.7 Simulated performance during starting  | 120 |
| Figure 5.8 Simulated performance; (a) System dynamics while acquiring near zero motor speed (b) System dynamics during speed reversal                           | 121 |
| Figure 5.9 Experimental performance; (a) Change in speed command (b) Acquisition of near zero rotor speed   | 122 |
| Figure 5.10 Experimental performance during speed reversal; (a) Torque and speed response (b) Phase reversal of stator currents                                 | 122 |
| Figure 5.11 Experimental performance during change in load torque   | 123 |

|   |     |
|---|-----|
| Figure 5.12 Simulated steady state performance of delta sigma modulator;  |     |
| (a) Load voltage control (b) Source current control   | 123 |
| Figure 5.13 Experimental steady state performance; (a) $dq$ plot of stator flux   |     |
| (b) Electromagnetic and load torque estimates (c) Reference and estimated speed   | 124 |
| Figure 5.14 Simulated harmonic performance; (a) Steady state stator current   |     |
| (b) Harmonic spectrum of stator current (c) Steady state source current at unity power factor (d) Harmonic spectrum of source current   | 125 |
| Figure 5.15 Experimental harmonic performance; (a) 3- $\phi$ steady state stator currents (b) Harmonic spectrum of stator current (c) Steady state source current at unity power factor (d) Harmonic spectrum of source current                   | 125 |
| Figure 5.16 System dynamic performance during starting; (a) With precise motor parameters (b) With 10% variation assumed in stator leakage inductance   | 126 |
| Figure 5.17 Experimental performance demonstrating motor control down to zero rotor speed; (a) Electromagnetic torque ( $T_e$ ), load torque estimate ( $T_L$ ) and rotor speed ( $N_r$ ) (b) 3- $\phi$ stator currents at different rotor speeds | 127 |
| Figure 5.18 Experimental performance during reversal in speed command; (a) Rotor speed reversal (b) Dynamics in stator current during speed reversal  | 127 |
| Figure 5.19 Simulated performance during load torque reversal   | 128 |
| Figure 5.20 Experimental performance during change in load torque   | 129 |
| Figure 5.21 Experimental steady state performance (a) $dq$ plot of rotor flux; (b) Estimated electro-magnetic torque ( $T_e$ ) and load torque ( $T_L$ ); (c) Predicted rotor speed ( $N_r$ ) and speed reference                                 | 130 |
| Figure 5.22 Simulated steady state harmonic performance (a) stator current profile and harmonic spectrum (b) source current profile and harmonic spectrum   | 130 |

|             |   |     |
|-------------|---|-----|
| Figure 5.23 | Experimental steady state harmonic performance; (a) 3- $\phi$ stator currents (b) Harmonic spectrum of stator current (c) Source current at near unity IPF with respect to source voltage (d) Harmonic spectrum of source current   | 131 |
| Figure 5.24 | CMV elimination using matrix converter; (a) Output phase voltages with respect to star point of the source and resulting CMV (b) CMV during device commutation  | 131 |
| Figure 5.25 | Comparative assessment of classical FS-MPC and FDM based MO-FS-MPC; (a) Dynamic response during change in load torque for classical weight based MO-FS-MPC (b) Dynamic response during change in load torque for FDM based MO-FS-MPC  | 133 |
| Figure 5.26 | Comparative assessment in terms of common mode voltage; (a) CMV performance with classical 21 states (b) CMV performance with only six states that trace a distinct input at each output.   | 134 |
| Figure 5.27 | Design of control gains $k_1$ and $k_2$ (a) $e_{\omega}^{p,u}$ for different values of $k_1$ , and $k_2 = 0$ (b) $e_{T_L}^{p,u}$ for different values of $k_2$ , and $k_1 = 150$ (c) $e_{\omega}^{p,u}$ for simultaneous variation of $k_1$ and $k_2$ (d) $e_{T_L}^{p,u}$ for simultaneous variation of $k_1$ and $k_2$ . | 135 |
| Figure 6.1  | 3 $\phi$ -3 $\phi$ (ABC-abc) matrix converter fed induction motor drive   | 138 |
| Figure 6.2  | VSI output line to neutral voltage vectors  | 140 |
| Figure 6.3  | Output line to neutral voltage vectors in a matrix converter  | 141 |
| Figure 6.4  | Input current vectors and corresponding switching states in a matrix converter  | 142 |
| Figure 6.5  | Block diagram of the proposed control algorithm   | 148 |
| Figure 6.6  | Block Diagram of open loop flux estimator and MRAC based closed-loop speed observer   | 151 |
| Figure 6.7  | Block Diagram for Direct Torque Control of Induction Motor using Space Vector Modulated Matrix Converter  | 153 |

|             |   |     |
|-------------|---|-----|
| Figure 6.8  | Space vector diagrams corresponding to output voltage (L-L) vectors and input current vectors   | 154 |
| Figure 6.9  | MATLAB/Simulink modeling for speed sensor-less hysteresis based DTC of 3- $\phi$ IMD using matrix converter using an adaptive observer  | 157 |
| Figure 6.10 | MATLAB/Simulink modeling for speed sensor-less DTC-SVM of 3- $\phi$ IMD using matrix converter using MRAS observer  | 157 |
| Figure 6.11 | Various estimated parameters during starting  | 159 |
| Figure 6.12 | Various system parameters during starting   | 160 |
| Figure 6.13 | System parameters during reversal of speed command  | 161 |
| Figure 6.14 | Experimental demonstration of speed reversal  | 161 |
| Figure 6.15 | System parameters during load perturbation  | 162 |
| Figure 6.16 | System dynamics during source perturbation  | 162 |
| Figure 6.17 | DQ variables for stator fluxes  | 163 |
| Figure 6.18 | Experimental DQ plot of stator flux   | 163 |
| Figure 6.19 | Experimental steady state waveforms for hysteresis based DTC; (a) Stator voltage and three-phase stator currents (b) Grid voltage and grid current at near unity power factor | 164 |
| Figure 6.20 | Experimental steady state waveforms; (a) Hysteresis control of torque (b) Reference and estimated rotor speed   | 164 |
| Figure 6.21 | Unfiltered source current and its harmonic spectrum   | 164 |
| Figure 6.22 | Filtered source current and its harmonic spectrum   | 165 |
| Figure 6.23 | Stator Flux, torque and speed estimation from stator voltage and sensed stator current  | 166 |
| Figure 6.24 | Dynamic behaviour of system parameters during starting  | 166 |
| Figure 6.25 | System Dynamics during speed reversal   | 167 |
| Figure 6.26 | Experimental steady state waveforms for DTC-SVM; (a) Stator voltage and three-phase stator currents (b) Grid voltage and grid current at near unity power factor              | 168 |

|             |  |     |
|-------------|--|-----|
| Figure 6.27 | Experimental steady state speed response and stator flux angle estimation  | 168 |
| Figure 6.28 | System Dynamics at varying speeds for (a) Conventional DTC; (b) DTC SVM  | 169 |
| Figure 6.29 | Unfiltered Source Current and its harmonic spectrum for (a) Conventional DTC; (b) DTC SVM  | 170 |
| Figure 7.1  | $1\phi$ - $3\phi$ matrix converter fed induction motor drive   | 173 |
| Figure 7.2  | Delta-Sigma Modulation for a $1\phi$ - $3\phi$ matrix converter  | 175 |
| Figure 7.3  | System block diagram for low speed sensor-less load oriented control of single-phase to three-phase matrix converter fed induction motor drive | 178 |
| Figure 7.4  | MATLAB/Simulink modeling for load side power quality improvement in $1\phi$ to $3\phi$ MC fed RL load, using delta sigma modulation.           | 179 |
| Figure 7.5  | MATLAB/Simulink modeling for speed sensor-less control of $1\phi$ to $3\phi$ MC fed IMD using MC with improved motor current quality.          | 180 |
| Figure 7.6  | Simulated dynamic performance of delta-sigma modulated $1\phi$ – $3\phi$ MC during load frequency change                                       | 182 |
| Figure 7.7  | Experimental dynamic performance of delta-sigma modulated $1\phi$ – $3\phi$ MC during load frequency change                                    | 182 |
| Figure 7.8  | Delta-Sigma Modulation for a $1\phi$ - $3\phi$ matrix converter  | 183 |
| Figure 7.9  | Simulated waveforms of source voltage, unfiltered and filtered source currents   | 183 |
| Figure 7.10 | Experimental waveforms of source voltage, unfiltered and filtered source currents  | 184 |
| Figure 7.11 | Simulated harmonic spectrum of load current for DSM modulated $1\phi$ – $3\phi$ MC.  | 184 |
| Figure 7.12 | Experimental harmonic spectrum of load current for DSM modulated $1\phi$ – $3\phi$ MC.   | 184 |
| Figure 7.13 | Simulated harmonic spectrum of filtered source current   | 185 |

|             |   |     |
|-------------|---|-----|
| Figure 7.14 | Experimental harmonic spectrum of filtered source current   | 185 |
| Figure 7.15 | Simulated starting performance of DSM modulated $1\phi$ - $3\phi$ MC fed IMD  | 186 |
| Figure 7.16 | Simulated system dynamics during speed control (100 rpm to near 0 rpm) in a DSM modulated $1\phi$ - $3\phi$ MC fed IMD  | 187 |
| Figure 7.17 | Experimental system dynamics during speed control (100 rpm to 45 rpm to 15 rpm) in a DSM modulated $1\phi$ - $3\phi$ MC fed IMD   | 188 |
| Figure 7.18 | Simulated system dynamics during speed reversal in a DSM modulated $1\phi$ - $3\phi$ MC fed IMD   | 188 |
| Figure 7.19 | Experimental system dynamics during speed reversal in a DSM modulated $1\phi$ - $3\phi$ MC fed IMD (a) Speed reversal (b) Phase reversal in stator currents                                       | 189 |
| Figure 7.20 | Simulated system dynamics during sudden withdrawal of load in DSM modulated $1\phi$ - $3\phi$ MC fed IMD  | 189 |
| Figure 7.21 | Experimental system dynamics during increase and subsequent decrease of load in DSM modulated $1\phi$ - $3\phi$ MC fed IMD  | 190 |
| Figure 7.22 | Simulated DQ plot of stator flux  | 191 |
| Figure 7.23 | Experimental DQ plot of stator flux   | 191 |
| Figure 7.24 | Experimental steady state performance of the drive (a) PWM load voltage and $3\phi$ motor currents (b) Reference and predicted motor speed (c) Load torque and predicted electro-magnetic torque. | 191 |
| Figure 7.25 | Stator current and its harmonic profile   | 192 |
| Figure 7.26 | Source current and its harmonic profile   | 192 |
| Figure 7.27 | Grid side harmonic performance (a) Source voltage and source current (b) Harmonic spectrum of $1\phi$ grid current  | 193 |
| Figure 8.1  | Desired waveforms in ideal $1\phi$ to $3\phi$ power conversion; (a) $1\phi$ source side parameters (b) $3\phi$ load side parameters   | 195 |
| Figure 8.2  | $1\phi$ - $3\phi$ matrix converter fed induction motor drive  | 196 |

|             |  |     |
|-------------|--|-----|
| Figure 8.3  | Performance of Kahn's modulation technique; (a) System parameters with resistive load (b) System parameters with inductive load                          | 197 |
| Figure 8.4  | MATLAB/Simulink modeling for implementation of Mo-FCS-MPC in 1- $\phi$ to 3- $\phi$ MC fed inductive load.   | 203 |
| Figure 8.5  | MATLAB/Simulink modeling for speed sensor-less Mo-FCS-MPC of 1- $\phi$ to 3- $\phi$ MC fed IMD.  | 204 |
| Figure 8.6  | Simulated dynamic performance during change in reference load current (or load voltage) amplitude; (a) SPWM (b) Load Oriented FCS-MPC (c) MO-FCS-MPC.    | 206 |
| Figure 8.7  | Simulated dynamic performance during change in reference load frequency from 5Hz to 10Hz; (a) SPWM (b) Load Oriented FCS-MPC (c) MO-FCS-MPC.             | 206 |
| Figure 8.8  | Experimental dynamic performance during change in reference load current (or load voltage) amplitude; (a) SPWM (b) Load Oriented FCS-MPC (c) MO-FCS-MPC. | 207 |
| Figure 8.9  | Experimental dynamic performance during change in reference load current frequency; (a) SPWM (b) Load Oriented FCS-MPC (c) MO-FCS-MPC.                   | 207 |
| Figure 8.10 | Simulated steady state performance; (a) SPWM (b) Load Oriented FCS-MPC (c) MO-FCS-MPC.   | 208 |
| Figure 8.11 | Experimental steady state performance on the load side; (a) SPWM (b) Load Oriented FCS-MPC (c) MO-FCS-MPC.   | 208 |
| Figure 8.12 | Experimental steady state performance on the source side; (a) SPWM (b) Load Oriented FCS-MPC (c) MO-FCS-MPC.   | 208 |
| Figure 8.13 | Simulated load side harmonic performance; (a) SPWM (b) Load Oriented FCS-MPC (c) MO-FCS-MPC.   | 209 |
| Figure 8.14 | Simulated source side harmonic performance; (a) SPWM (b) Load Oriented FCS-MPC (c) MO-FCS-MPC.   | 209 |

|             |   |     |
|-------------|---|-----|
| Figure 8.15 | Experimental source side harmonic performance; (a) SPWM (b) Load Oriented FCS-MPC (c) MO-FCS-MPC.   | 210 |
| Figure 8.16 | Source current displacement with respect to source voltage; (a) SPWM (b) Load Oriented FCS-MPC (c) MO-FCS-MPC.  | 210 |
| Figure 8.17 | Starting performance of MO-FCS-MPC based 1- $\phi$ to 3- $\phi$ MC fed IMD (a) Starting with MO-FCS-MPC (b) Starting with single objective load oriented FCS-MPC, followed by switching over to MO-FCS-MPC. | 212 |
| Figure 8.18 | Dynamic performance of MO-FCS-MPC based 1- $\phi$ to 3- $\phi$ MC fed IMD   | 213 |
| Figure 8.19 | Experimental performance of MO-FCS-MPC based 1- $\phi$ to 3- $\phi$ MC fed IMD  | 213 |
| Figure 8.20 | Steady state performance of MO-FCS-MPC based 1- $\phi$ to 3- $\phi$ MC fed IMD  | 214 |
| Figure 8.21 | Steady state performance of MO-FCS-MPC based 1- $\phi$ to 3- $\phi$ MC fed IMD (a) Torque response (b) Speed Response (c) DQ plot of rotor flux   | 214 |
| Figure 8.22 | Motor side power quality assessment in MO-FCS-MPC based 1- $\phi$ to 3- $\phi$ MC fed IMD   | 215 |
| Figure 8.23 | Source side power quality assessment in MO-FCS-MPC based 1- $\phi$ to 3- $\phi$ MC fed IMD (a) Source current and its harmonic spectrum (b) Operation near unity input power factor.                        | 216 |
| Figure 8.24 | Experimental waveform on the motor side   | 216 |
| Figure 8.25 | Source side power quality assessment in MO-FCS-MPC based 1- $\phi$ to 3- $\phi$ MC fed IMD (a) Source current at near unity input power factor. (b) Harmonic spectrum of source current                     | 216 |

# List of Tables

|            |  |     |
|------------|--|-----|
| Table 3.1  | Induction Motor Parameters   | 36  |
| Table 4.1  | Switching States and resulting CMV in Matrix Converter   | 48  |
| Table 4.2  | Example of Switching Table Generation from Sector Information  | 55  |
| Table 4.3  | Example of Load Voltage Modulator (LVM) Implementation using DSM for Group-I and Group-II vectors                | 59  |
| Table 4.4  | Example of Source Current Modulator (SCM) Implementation using DSM for Group-I and Group-II vectors              | 61  |
| Table 4.5  | LVM Switching Implementation for Load Voltage Control for Group-III vectors                                      | 68  |
| Table 4.6  | SCM Switching Implementation for Source Current Control for Group-III vectors                                    | 70  |
| Table 4.7  | System Parameters and Their Specifications   | 74  |
| Table 4.8  | Choice of Control Parameter ‘ $n$ ’  | 79  |
| Table 4.9  | System Parameters used in Simulation/Experimentation   | 80  |
| Table 4.10 | System Specifications  | 85  |
| Table 4.11 | Comparison of proposed PDSM technique with other modulation schemes for MCs                                      | 90  |
| Table 4.12 | Comparative performance of existing modulation techniques for Group-III vectors                                  | 92  |
| Table 5.1  | Load Voltage Control (LVC) through DSM   | 105 |
| Table 5.2  | Source Current Control (SCC) Through DSM   | 106 |
| Table 5.3  | Zero CMV states in Matrix Converter  | 107 |
| Table 5.4  | Comparison between harmonic performance of classical FS-MPC and FDM based FS-MPC at different loading conditions | 133 |
| Table 6.1  | Switching Table For DTC  | 141 |

|           |   |     |
|-----------|---|-----|
| Table 6.2 | Switching Combinations and Resultant Space Vectors in a MC                                    | 143 |
| Table 6.3 | Switching Table for DTC via MC incorporating PFC  | 144 |
| Table 6.4 | Switching Combinations and Resultant Space Vectors in a MC                                    | 155 |
| Table 6.5 | Example of Switching Table Generation for SVM with IPF control                                | 156 |
| Table 6.6 | Source Current Parameters at varying motor speeds in conventional<br>DTC and DTC SVM          | 170 |
| Table 7.1 | Switching Combinations for a $1\phi - 3\phi$ MC   | 176 |
| Table 7.2 | Example of Decisional Element Implementation in Delta-Sigma Mod-<br>ulated $1\phi - 3\phi$ MC | 177 |
| Table 7.3 | System Specifications For Delta Sigma Modulation in $1\phi-3\phi$ MC                          | 181 |
| Table 8.1 | Switching States in 1t3-MC  | 200 |
| Table 8.2 | Specifications of System Parameters   | 205 |